The Plant Cell, Vol. 18, 1833–1845, August 2006, www.plantcell.org © 2006 American Society of Plant Biologists

Functional Analyses of Two Tomato *APETALA3* Genes Demonstrate Diversification in Their Roles in Regulating Floral Development[W]

Gemma de Martino,[a] Irvin Pan,[a] Eyal Emmanuel,[b] Avraham Levy,[b] and Vivian F. Irish[a,c,1]

[a] Department of Molecular, Cellular, and Developmental Biology, Yale University, New Haven, Connecticut 06520
[b] Department of Plant Sciences, Weizmann Institute of Sciences, Rehovot, Israel 76100
[c] Department of Ecology and Evolutionary Biology, Yale University, New Haven, Connecticut 06520

The floral homeotic *APETALA3* (*AP3*) gene in *Arabidopsis thaliana* encodes a MADS box transcription factor required for specifying petal and stamen identities. *AP3* is a member of the *euAP3* lineage, which arose by gene duplication coincident with radiation of the core eudicots. Although *Arabidopsis* lacks genes in the paralogous *Tomato MADS box gene 6* (*TM6*) lineage, tomato (*Solanum lycopersicum*) possesses both *euAP3* and *TM6* genes, which have functionally diversified. A loss-of-function mutation in *Tomato AP3* (*TAP3*) resulted in homeotic transformations of both petals and stamens, whereas RNA interference–induced reduction in *TM6* function resulted in flowers with homeotic defects primarily in stamens. The functional differences between these genes can be ascribed partly to different expression domains. When overexpressed in an equivalent domain, both genes can partially rescue the *tap3* mutant, indicating that relative levels as well as spatial patterns of expression contribute to functional differences. Our results also indicate that the two proteins have differing biochemical capabilities. Together, these results suggest that *TM6* and *TAP3* play qualitatively different roles in floral development; they also support the ideas that the ancestral role of *AP3* lineage genes was in specifying stamen development and that duplication and divergence in the *AP3* lineage allowed for the acquisition of a role in petal specification in the core eudicots.

INTRODUCTION

Gene duplication can provide the raw material for the evolution of new functions. This can occur by subfunctionalization (partitioning of the original gene function into two parts) or by neofunctionalization (acquisition of a new role by one of the duplicates), and such changes are thought to contribute to the retention of both duplicated genes in the genome (Ohno, 1970; Force et al., 1999; Lynch and Conery, 2000; Lynch and Force, 2000). Traditionally, researchers have examined the adaptive significance of the retention of duplicate gene pairs by characterizing patterns of nucleotide substitutions within coding regions (Lynch and Conery, 2000). By contrast, relatively little work has been performed to assess the functional consequences of gene duplication and diversification. Here, we explore the degree to which coding versus regulatory changes have contributed to differences in gene function in duplicate genes belonging to the floral homeotic *APETALA3* (*AP3*) lineage.

The *AP3* lineage genes are a subfamily of the large MADS box family of transcription factors, which have been implicated in the regulation of a number of plant developmental processes (Irish and Kramer, 1998; Theissen et al., 2000). A major gene duplication event in the *AP3* gene lineage has led to two paralogous lineages, the *euAP3* and the *Tomato MADS box gene 6* (*TM6*) gene lineages, in the core eudicot clade of the angiosperms (Kramer et al., 1998; Kramer and Irish, 1999), which suggests that this gene duplication occurred ~125 million years ago (Magallon et al., 1999). The core eudicot *TM6* lineage contains sequence motifs similar to those of the ancestral *paleoAP3* lineage genes, whereas the *euAP3* lineage genes possess a set of different sequence motifs and so represent a divergent paralogous lineage (Kramer et al., 1998). In particular, the *TM6* and *euAP3* lineage gene products are distinguished by different C-terminal domains, which likely arose by an ancestral frameshift mutation (Kramer et al., 1998, 2006; Vandenbussche et al., 2003).

Within the core eudicots, all functionally characterized *AP3* genes belong to the divergent *euAP3* lineage. These include the well-characterized *Arabidopsis thaliana AP3* and *Antirrhinum majus DEFICIENS* (*DEF*) genes, both of which have been shown to play key roles in the specification of petal and stamen identities (Bowman et al., 1989; Carpenter and Coen, 1990; Sommer et al., 1990; Jack et al., 1994). Consistent with this role, both *AP3* and *DEF* are expressed in petal and stamen primordia, and their expression in these organs persists through later stages of differentiation. However, there are some differences in the patterns of expression of these genes in their respective species. For instance, *Antirrhinum DEF* is also transiently expressed in the carpel primordia, whereas *Arabidopsis AP3* is additionally expressed in a small adaxial patch of sepal cells (Jack et al., 1992; Schwarz-Sommer et al., 1992).

[1] To whom correspondence should be addressed. E-mail vivian.irish@yale.edu; fax 203-432-5711.
The author responsible for distribution of materials integral to the findings presented in this article in accordance with the policy described in the Instructions for Authors (www.plantcell.org) is: Vivian F. Irish (vivian.irish@yale.edu).
[W]Online version contains Web-only data.
Article, publication date, and citation information can be found at www.plantcell.org/cgi/doi/10.1105/tpc.106.042978.

Members of the *PISTILLATA* (*PI*) subfamily of MADS box genes have also been shown to be required for petal and stamen specification (Bowman et al., 1989; Trobner et al., 1992; Goto and Meyerowitz, 1994). In *Arabidopsis*, the PI and AP3 proteins heterodimerize, which appears to be necessary for DNA binding and stable localization of this transcription factor complex to the nucleus (McGonigle et al., 1996; Riechmann et al., 1996a, 1996b). Furthermore, the AP3/PI heterodimeric complex has been shown to be responsible for the continued expression of both *AP3* and *PI* through a positive feedback loop (Jack et al., 1992, 1994; Goto and Meyerowitz, 1994; Honma and Goto, 2000). This transcriptional complex likely includes other proteins, because AP3 and PI also physically interact with the MADS box proteins AP1 and SEP3 (Honma and Goto, 2001). The formation of distinct MADS box protein complexes in different floral organ whorls has been postulated to be responsible for organ-type specific differentiation (Honma and Goto, 2001; Pelaz et al., 2001; Theissen and Saedler, 2001). Similarly, the *Antirrhinum PI* lineage gene product, *GLOBOSA* (*GLO*), must heterodimerize with *DEF* to bind to DNA (Schwarz-Sommer et al., 1992; Trobner et al., 1992) and also forms larger MADS box protein complexes that are thought to specify organ-type differentiation (Davies et al., 1996b). However, functional analyses of the two *Petunia hybrida PI* ortholog genes, *FBP1* (also known as Ph *GLO1*) and *pMADS2* (Ph *GLO2*), as well as protein interaction data suggest that in *Petunia*, petal and stamen identities are specified by protein complexes that are qualitatively distinct from their *Arabidopsis* counterparts and whose abundance is believed to be critical for proper organ development (Vandenbussche et al., 2004). These results suggest that there is some plasticity to the types of MADS box protein complexes formed and their functions in planta.

In contrast with the *euAP3* lineage, functional characterization of *TM6* lineage genes has not yet been performed in any species. Several lines of evidence have suggested that *TM6* lineage genes may play a role in stamen specification and/or differentiation. In *Petunia*, loss-of-function mutations in the *euAP3* gene Ph *DEF* (also known as *GP* and *pMADS1*) only affect the specification of petals (van der Krol et al., 1993; Halfter et al., 1994; Tsuchimoto et al., 2000; Vandenbussche et al., 2004). Stamen identity is thought to be dependent on the action of another MADS box gene (Tsuchimoto et al., 2000), a likely candidate being the *TM6* representative Ph *TM6*, because it is highly expressed in the third and fourth whorls (Vandenbussche et al., 2004). It has also been shown that a chimeric cDNA, containing a C-terminal *paleoAP3* motif characteristic of *paleoAP3* or *TM6* lineage genes, fused in frame to an *Arabidopsis AP3* cDNA, is sufficient to largely rescue stamen but not petal development of *Arabidopsis ap3* mutant flowers (Lamb and Irish, 2003). Together, these data suggest that the core eudicot *TM6* lineage genes function predominantly in stamen development, although this has not yet been critically tested. Based on these observations, we previously suggested that the advent of the divergent *euAP3* lineage genes may be correlated with the de novo evolution of petals in the core eudicots (Kramer and Irish, 1999, 2000; Irish, 2003).

Here, we characterize the functions of the tomato (*Solanum lycopersicum*) *TM6* (*TM6*) and *euAP3* (*Tomato APETALA3* [*TAP3*]) genes to parse the relative contributions of these gene duplicates to specifying petal and stamen development in this species. We describe loss-of-function phenotypes for *TM6* and *TAP3* that indicate that these tomato genes play distinct roles in flower development, with *TAP3* required to specify both petal and stamen identity, whereas *TM6* appears to play a role predominantly in stamen differentiation. The data we present indicate that both changes in expression and changes in protein coding functions have likely contributed to the differences in the roles of *TM6* and *TAP3*. These results also support the idea that the divergent *euAP3* lineage genes have been redeployed to a role in petal specification in the core eudicots. Surprisingly, similar analyses of the *TM6* and *euAP3* lineage genes in the closely related species *P. hybrida* indicate that these paralogous genes have subfunctionalized their roles in a different way (van der Krol et al., 1993; Tsuchimoto et al., 2000; Rijpkema et al., 2006). Together, these data demonstrate that paralogous gene duplicates can take on different roles in different lineages, illustrating the dynamic and fluid nature of subfunctionalization.

RESULTS

Identification and Phylogenetic Analyses of *AP3* Lineage Genes in Tomato

Using rapid amplification of cDNA ends (RACE), we identified the full-length coding sequence of *TAP3*; a partial *TAP3* sequence and the coding sequence of *TM6* have been published previously (Pnueli et al., 1991; Kramer et al., 1998). To place these sequences in a phylogenetic context, we performed phylogenetic analyses using neighbor joining of eudicot *AP3* lineage genes and the predicted amino acid sequences of the MIK domains (Figure 1). These results confirm the placement of the tomato *TM6* gene in the *TM6* clade and tomato *TAP3* in the *euAP3* clade (Kramer et al., 1998; Kramer and Irish, 2000; Vandenbussche et al., 2003). *TM6* is most closely related to *TM6* representatives from other Solanales species, including *P. hybrida TM6* and *Nicotiana tabacum TM6*, within a larger clade of core eudicot *TM6* genes. Similarly, *TAP3* groups together with *euAP3* representatives from other Solanales species within the core eudicot *euAP3* clade. These observations support the hypothesis that the duplication resulting in the *TM6* and *euAP3* lineages occurred coincidentally with the diversification of the core eudicots (Kramer et al., 1998; Kramer and Irish, 2000; Vandenbussche et al., 2003; Kim et al., 2004; Stellari et al., 2004). Furthermore, examination of the extant EST collection for tomato (http://www.sgn.cornell.edu/index.pl) does not reveal any other *AP3* lineage genes, nor have we identified any other *AP3*-related genes in tomato via degenerate RT-PCR or by DNA gel blot hybridization analyses (data not shown). As such, it appears that tomato possesses a single *euAP3* lineage gene, *TAP3*, and a single *TM6* lineage gene, *TM6*.

Identification of Loss-of-Function Lines for *TAP3* and *TM6*

To characterize the function of *AP3* lineage genes in tomato, we screened Ds insertion lines (Meissner et al., 1997, 2000) for phenotypes likely to reflect a mutation in an *AP3* lineage gene. One such mutation was identified and shown to correspond to an insertion in the first exon of the *TAP3* gene (Figure 2A). As

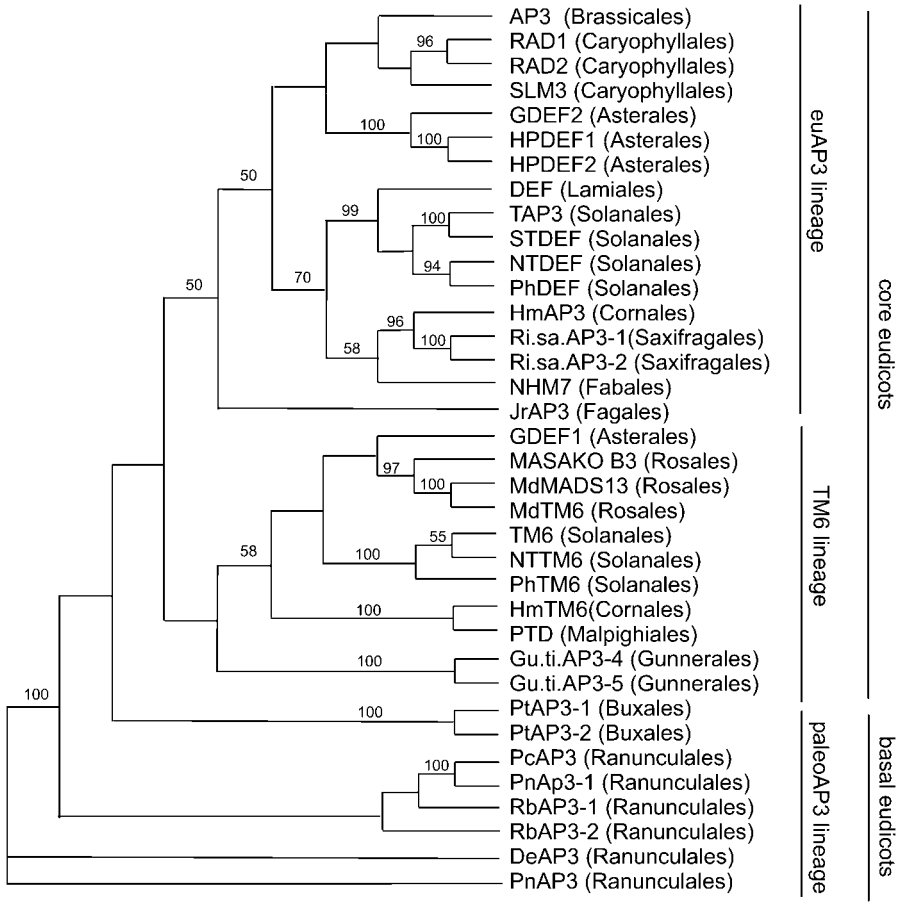

Figure 1. Neighbor-Joining Analysis of *euAP3* and *TM6* Lineage Genes.

Representative *AP3* lineage genes from core eudicots and basal eudicots were included in the analysis; the basal eudicot Pn *AP3* gene was used as the outgroup. Bootstrap values of ≥50% are shown.

expected, the expression of the *TAP3* gene in the insertional mutant was completely abolished (Figure 2C). Because we did not recover any insertional mutations in the *TM6* gene, we resorted to using an RNA interference (RNAi) approach to generate a loss-of-function phenotype. An RNAi construct was designed to target the last 200 nucleotides of the *TM6* transcript (Figure 2B). Eight loss-of-function TM6i transgenic lines were generated, and *TM6* expression was strongly reduced in all eight lines (Figure 2D). The RNAi-induced gene silencing of *TM6* was gene-specific, in that transcript levels of the closest paralog, *TAP3*, were unaffected (Figure 2E).

tap3 and TM6i Loss-of-Function Lines Affect Different Aspects of Flower Development

Normal tomato flowers (cv Micro-Tom) contain five or six sepals, alternating with five to six yellow petals; the reproductive organs consist of five yellow stamens forming a cone, which enclose two fused carpels that develop a multilocular ovary and a protruding style and stigma (Figure 3A). Each organ type displays characteristic epidermal cell types (Figures 3B to 3I). Wild-type sepals contain stomata and trichomes on the adaxial surface (Figure 3B). In the second whorl, the adaxial epidermis of the petals contains rounded cells, whereas the abaxial surface contains epidermal cells that are more elongate as well as sparse trichomes (Figures 3C and 3D). In the third whorl, a row of lateral and adaxial trichome hairs present on adjacent stamens interweave to form the staminal cone (Sekhar and Sawhney, 1984) (Figure 3E). The proximal regions of the anthers contain multilobed epidermal cells, whereas the epidermal cells are more elongated in the distal regions (Figures 3F and 3G). In the carpels, the epidermal cells are rounded in the proximal region and elongated in the distal region (Figures 3H and 3I).

In contrast with the wild type, *tap3* homozygous mutant plants develop flowers showing a classic B-class gene loss-of-function phenotype consisting of a complete transformation of the petals into sepalloid structures and stamens into carpel-like organs (Figure 3J). Scanning electron microscopy confirmed the homeotic conversion of the epidermal cells of these organs (Figures 3L, 3M, 3O, and 3P). In the second whorl, the epidermal cells had a sepal-like epidermal morphology, and stomata were observed on both the abaxial and adaxial surfaces (Figures 3L and 3M).

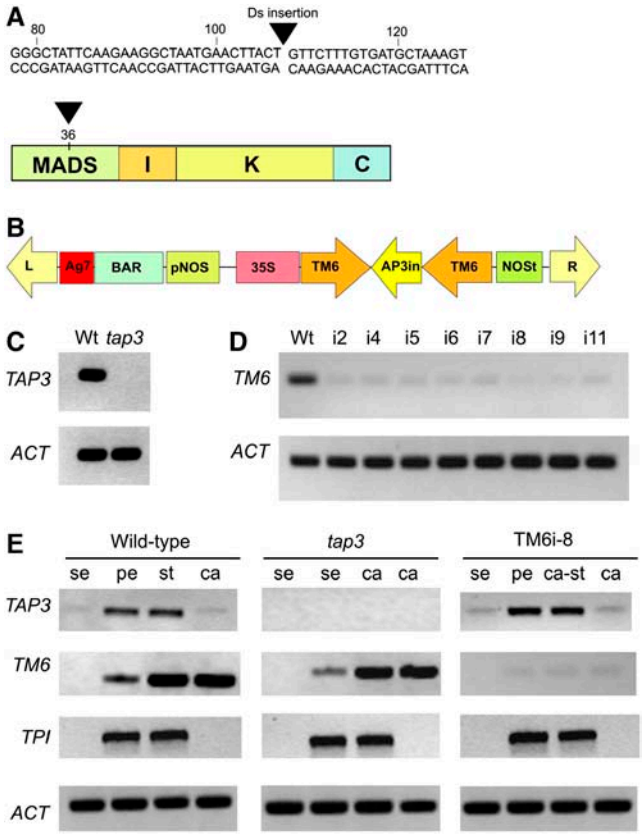

Figure 2. Characterization of Loss-of-Function Lines for *TAP3* and *TM6*.

(A) Location of the insertion of a Ds element in the first exon of *TAP3* at position +108 within the MADS domain.
(B) pTCSH1-TM6 RNAi construct used for RNAi-induced silencing of the *TM6* gene.
(C) RT-PCR using *TAP3*-specific primers on wild-type and *tap3* inflorescence tissue (stages 9 to 18); no amplification could be detected in the *tap3* tissue. Amplification of the tomato *ACTIN* gene (*ACT*) was used as a control.
(D) RT-PCR using TM6-specific primers on wild-type and TM6i lines. Flowers from stages 15 to 20 showing a strong phenotype were analyzed for all transgenic lines. As expected, the level of the *TM6* transcript was highly reduced in the transgenic lines.
(E) RT-PCR analyses to determine the organ-specific expression of *TAP3*, *TM6*, and *TPI* genes in wild-type, *tap3* mutant, and *TM6i8* transgenic lines. Floral organs were dissected from stage 9 to 18 flowers and pooled, and the resulting RNA was used for RT-PCR. se, sepals; pe, petals; st, stamens; ca, carpels; ca-st, carpelloid stamens.

The third whorl organs, instead of forming a cone as in the wild type, were splayed out and appeared carpelloid (Figure 3N); the third whorl carpel-like epidermal cells were indistinguishable from those of normal fourth whorl wild-type carpels (Figures 3O and 3P). The third whorl carpelloid structures produced ectopic fruit lobes that did not contain normal locules and lacked seeds (data not shown). The first and fourth whorl organs of *tap3* mutant flowers appeared to be normal (Figures 3K, 3Q, and 3R). Dissection of the *tap3* fourth whorl carpels revealed the presence of normal ovules that were able to set seeds when manually pollinated with wild-type pollen (data not shown).

The phenotypes produced by the TM6i5, TM6i6, TM6i8, and TM6i9 lines were characterized in detail (Tables 1 and 2, Figures 3S to 3AB). The TM6i8 and TM6i9 lines showed a more extreme phenotype in which 91 to 96% of flowers developed carpelloid stamens (Table 1, Figure 3S). The epidermal cells of these transgenic third whorl organs were smaller and arranged differently from the interlocking arrangement of comparable wild-type cells (cf. Figures 3F and 3Y). Furthermore, cells with an aberrant morphology developed in the epidermis of the proximal region of these third whorl organs (Figure 3W, inset). Third whorl organ fusion was often incomplete, as a result of the absence of interweaving lateral hairs in the proximal region (Figure 3W).

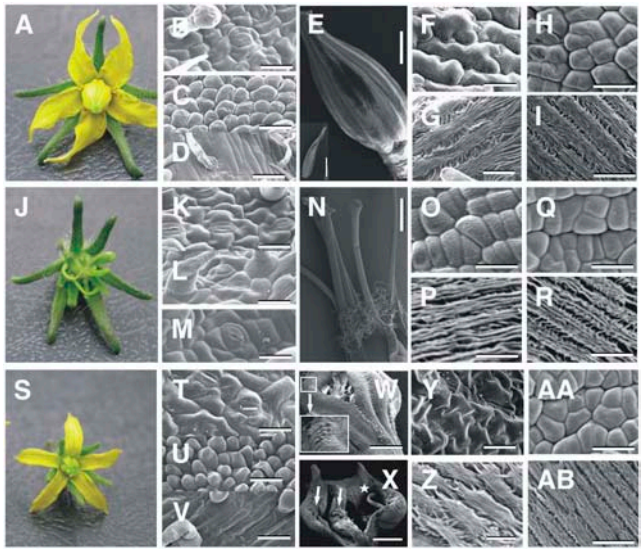

Figure 3. Phenotypic Analyses of the *tap3* Mutant and the *TM6i-8* Line.

Light and scanning electron microscopy of wild-type (Micro-Tom) flowers (**[A]** to **[I]**), *tap3* flowers (**[J]** to **[R]**), and *TM6i-8* flowers (**[S]** to **[AB]**).
(B), **(K)**, and **(T)** Adaxial epidermal cells of the first whorl organs.
(C), **(L)**, and **(U)** Adaxial epidermal cells of the second whorl organs.
(D), **(M)**, and **(V)** Abaxial epidermal cells of the second whorl organs.
(E) Wild-type staminal cone. The inset shows the adaxial surface of the anther.
(N) *tap3* third whorl organs showing carpel-like morphology.
(W) Abaxial view of a *TM6i-8* staminal cone showing partial lateral fusion (inset).
(X) Adaxial view of a *TM6i-8* carpelloid stamen showing naked ovules (arrows) and stigmatic tissue (star).
(F), **(O)**, and **(Y)** Abaxial epidermal cells of the proximal region of the third whorl organs.
(G), **(P)**, and **(Z)** Abaxial epidermal cells of the distal region of the third whorl organs.
(H), **(Q)**, and **(AA)** Epidermal cells of the proximal region of the fourth whorl organs.
(I), **(R)**, and **(AB)** Epidermal cells of the distal region of the fourth whorl organs.
Bars = 40 μm (**[B]**, **[C]**, **[G]** to **[I]**, **[K]** to **[M]**, **[O]** to **[R]**, **[T]**, **[U]**, **[Z]**, **[AA]**, and **[AB]**), 90 μm (**[D]**, **[F]**, and **[V]**), 20 μm **(Y)**, 2 mm (inset in **[E]** and **[N]**), 1 mm (**[W]** and **[X]**), and 1.5 mm **(E)**.

Table 1. Quantification of Third Whorl Floral Phenotypes of Four TM6i Lines

Lines	Class 0	Class 1	Class 2	Class 3
Wild type ($n = 200$)	99.9%	0.1%	0%	0%
TM6i5 ($n = 372$)	24.0%	47.0%	25%	4%
TM6i6 ($n = 418$)	21.0%	28.0%	38%	13%
TM6i8 ($n = 474$)	9.0%	5.0%	10%	76%
TM6i9 ($n = 450$)	4.0%	7.0%	22%	67%

Phenotypes were grouped in four classes: class 0 consists of flowers with normal phenotype; class 1 consists of flowers with only one stamen displaying carpelloidy; class 2 consists of flowers with two to four carpelloid stamens; and class 3 consists of flowers with all carpelloid stamens.

Often, naked ovules developed on the adaxial face of these third whorl organs (Figure 3X). Transgenic TM6i flowers with an extreme transformation of stamens to carpelloid tissue were male-sterile, but seeds developed normally when such flowers were manually crossed with wild-type pollen. This observation indicates that the ovules of such transgenic plants were functional. When not pollinated, sterile parthenocarpic fruits developed.

Petals of the transgenic TM6i plants were also affected in terms of overall size (Table 2). The reduction in petal size was probably caused by a decrease in cell proliferation, because similar cell sizes were observed in these lines compared with the wild type (cf. Figures 3C and 3U). Furthermore, the second whorl organs of TM6i lines did not display any apparent homeotic conversions, in that they displayed normal epidermal cell types across the petal (Figures 3U and 3V).

Despite the high levels of expression of the *TM6* gene in ovules and during fruit development in wild-type flowers (see below), reduction in its expression did not seem to interfere with the normal differentiation of fourth whorl organs. Transgenic TM6i carpel tissue appeared normal, as did the sepals (Figures 3T, 3AA, and 3AB).

TAP3 and *TM6* Are Expressed in Distinct but Overlapping Domains in the Flower

To determine whether the differences in *TM6* and *TAP3* function could be ascribed to different domains of expression, we examined their spatial and temporal patterns of expression. Floral organs were dissected from flowers at stages 9 to 18 of development (tomato flower stages according to Brukhin et al. [2003]), and the individual organ types were pooled and used in RT-PCR experiments (Figure 2E). *TAP3* expression could be detected at high levels in petals and stamens. *TM6*, by contrast, was expressed predominantly in stamens and carpels, with some expression detected in petals. This pattern of *TM6* expression is similar to what has been reported previously (Pnueli et al., 1991; Lozano et al., 1998; Busi et al., 2003). We also compared these patterns with the expression pattern of the *Tomato PISTILLATA* gene (*TPI*), which we identified using an RT-PCR–based approach (see Methods). *TPI* transcripts were detected almost exclusively in the petals and stamens.

To further characterize these patterns of expression at early stages of floral development (before stage 9), we performed in situ hybridizations for *TAP3*, *TM6*, and *TPI* (Figure 4). *TAP3* expression was first seen in presumptive petal primordia (Figure 4A), and by stage 3 it could be detected throughout the petal and in the subepidermal cells of stamen primordia (Figure 4B). Expression of *TAP3* in petal and stamen primordia persisted until later stages of floral development (Figure 4C), and by stage 9 (Figure 4D) it was restricted to particular tissues in the differentiating petals and stamens. In stage 9 stamens, *TAP3* expression was largely confined to the vascular bundle and tapetal cells of the stamen and to the lateral edges of the petals. The low levels of *TAP3* expression in sepals and carpels detected by RT-PCR (Figure 2E) were not observed by in situ hybridization, presumably because of the low levels of expression in these tissues or the different stages of flower development used in the two analyses. The pattern of *TAP3* expression contrasts with what we observed for *TM6* expression. At stage 2, *TM6* expression was more ubiquitous, throughout the petal, stamen, and carpel primordia (Figure 4E). This pattern of expression persisted through stage 3 (Figure 4F) and stage 5 (Figure 4G). By stage 9, *TM6* expression was most prominent in the inner integuments of the developing ovules and also could be detected in the lateral margins of the developing petals (Figure 4H). As such, the patterns of expression of *TAP3* and *TM6* overlap considerably at the earliest stages of floral development but become restricted to largely distinct spatial domains within the developing flower bud by stage 9. Later in floral development (in stage 9 to 18 flowers), *TM6* expression appears to become more prominent in the stamens and carpels (Figure 2E).

By contrast, the pattern of expression of *TPI* was more similar to that of *TAP3. TPI* expression was similar to that of *TAP3* at stage 2, in the presumptive petal primordia (Figure 4I). *TPI* expression could be detected in developing petal and stamen primordia at stages 4 (Figure 4J) and 5 (Figure 4K). By stage 9, *TPI* expression was restricted to particular tissues of the developing petals and stamens, with expression seen in the lateral edges of the petals and at high levels in the tapetal cells of the stamen (Figure 4L).

TAP3, Le *TM6*, and *TPI* Regulatory Interactions

To determine whether the *tap3* mutation resulted in coordinate downregulation of either the *TM6* or *TPI* gene, we examined the

Table 2. Petal Size Quantification of the TM6 RNAi Line Floral Classes

Class	pl = 1.07 ± 0.09 pw = 0.40 ± 0.05	pl = 0.85 ± 0.07 pw = 0.36 ± 0.02	pl = 0.52 ± 0.04 pw = 0.21 ± 0.02
Class 0 ($n = 43$)	97%	3%	0%
Class 1 ($n = 38$)	95%	5%	0%
Class 2 ($n = 45$)	15%	58%	27%
Class 3 ($n = 45$)	0%	13%	87%

Correlation of petal size with the degree of stamen transformation in the TM6i flowers. pl, mean petal length ± SE; pw, mean petal width ± SE. Petal length and width (in centimeters) were measured for each class; the floral classes are defined in Table 1.

Figure 4. In Situ Expression Analyses of *TAP3*, *TM6*, and *TPI*.

Expression in wild type (Micro-Tom) flower buds of *TAP3* (**[A]** to **[D]**), *TM6* (**[E]** to **[H]**), and *TPI* (**[I]** to **[L]**).
(A) *TAP3* expression is apparent by stage 2, with expression seen predominantly in the petal primordia.
(B) By stage 3, expression can be seen throughout the petal primordia as well as in the subepidermal cell layers of the incipient stamen primordia (arrowhead).
(C) *TAP3* expression in the petal and stamen primordia (arrowhead) at stage 5.
(D) Cross section of a flower at stage 9. *TAP3* expression becomes restricted to the vascular bundle and tapetal cells of the stamens, whereas expression in the petals is seen in the lateral edges (arrowhead).
(E) Relatively low levels of *TM6* expression can be seen at stage 2 throughout the presumptive petal, stamen, and carpel primordia.
(F) and **(G)** This pattern of expression persists through stage 3 **(F)** and stage 5 **(G)**.
(H) By stage 9, *TM6* expression is most prominent in the developing ovules, localized predominantly to the inner integuments (inset). Low levels of expression can also be detected in the lateral margins of the petals (arrowhead).
(I) *TPI* expression can be detected by early stage 2 in the presumptive petal primordia.
(J) and **(K)** *TPI* expression is observed in developing petal and stamen primordia at stage 4 **(J)** and stage 5 **(K)**.
(L) By stage 9, *TPI* expression is seen mainly in the stamens, with high levels of expression in the tapetal cells. *TPI* expression can also be detected in the lateral margins of the petals (arrowhead).

expression of these genes in the *tap3* mutant background (Figure 2E). The levels and patterns of expression of both *TM6* and *TPI* transcripts in the *tap3* mutant flowers were similar to those of wild-type flowers, indicating that *TAP3* is not required for the expression of these genes. This is in contrast with the situation in *Arabidopsis*, in which *AP3* is required for the maintenance of *PI* gene expression (Goto and Meyerowitz, 1994; Honma and Goto, 2000). Similarly, downregulation of *TM6* expression in the TM6i8 line had no effect on the expression levels or patterns of *TAP3* or *TPI* (Figure 2E). These results demonstrate that the dramatic loss-of-function phenotype produced by the *tap3* mutant is not attributable to coordinate downregulation of *TM6* and that expression of the endogenous *TM6* gene is not able to compensate for the loss of *TAP3* function in petal and stamen development. Similarly, the phenotypes we observed for RNAi-induced loss of *TM6* function are not the result of the coordinate loss of either *TAP3* or *TPI* expression. Thus, *TAP3* and *TM6* have distinct functions in flower development.

TM6 and *TAP3* Play Similar Roles When Ectopically Expressed

The complete loss of petals and stamens in the *tap3* mutant suggests that the endogenous level of *TM6* expression is not sufficient to compensate for the loss of *TAP3* function. In wild-type flowers, in fact, *TM6* appears to be expressed at a lower level than *TAP3*, based on RNA gel blot and in situ hybridization analyses (Figure 4; data not shown). To test whether levels or domains of expression were critical for differences in *TM6* and *TAP3* function, we overexpressed the *TAP3* and *TM6* genes in the *tap3* mutant. We generated transgenic lines in which the *AP3* or *TM6* coding region was driven by the strong constitutive 35S promoter (Benfey and Chua, 1990) and introduced these constructs into a *leap3* homozygous mutant background. Two transgenic lines were obtained for each construct. Both *35S:TAP3* and *35S:TM6* were able to rescue the *tap3* second whorl phenotype to somewhat different degrees (Figures 5B, 5C, 5G, and 5H). In both *35S:TM6;tap3* and *35S:TAP3;tap3* lines, the second whorl adaxial epidermis consisted of both sepal- and petal-like cells. Although stomata were still observed in the second whorl organs in the *35S:TAP3;tap3* flowers, these chimeric organs did not develop trichomes on the adaxial surface, indicating that *TAP3* was able to better rescue the second whorl than *TM6* (Figure 5G). The rescue of the *tap3* third whorl phenotype by either *35S:TAP3* or *35S:TM6* was much more limited in

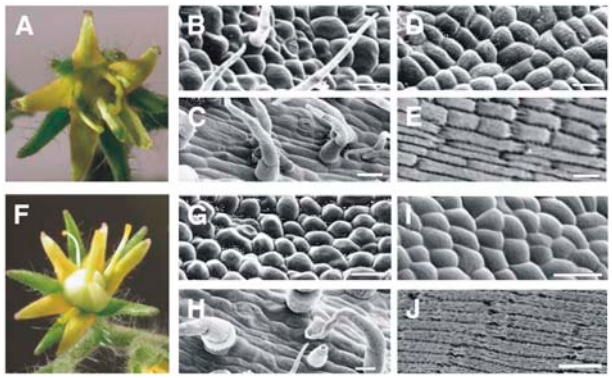

Figure 5. Rescue of the Phenotype Conferred by *tap3* by Overexpression of *TM6* or *TAP3*.

(A) *35S:TM6;tap3* flower.
(B) and **(C)** Adaxial **(B)** and abaxial **(C)** epidermal cells of the *35S:TM6;tap3* second whorl organs.
(D) and **(E)** Epidermal cells of proximal **(D)** and distal **(E)** regions of third whorl organs of the *35S:TM6;tap3* flower.
(F) *35S:TAP3;tap3* flower.
(G) and **(H)** Adaxial **(G)** and abaxial **(H)** epidermal cells of the *35S:TAP3;tap3* second whorl organs.
(I) and **(J)** Epidermal cells of proximal **(I)** and distal **(J)** regions of third whorl organs of the *35S:TAP3;tap3* flower.
Bars in scanning electron micrographs = 20 μm.

that these organs largely displayed cell morphologies typical of carpel epidermal cells (Figures 5D, 5E, 5I, and 5J).

To check whether the failure in the rescue of the third whorl was attributable to a lack of transgene expression in the third whorl organs, we performed RT-PCR with transgene-specific primers using dissected second and third whorl tissues (see Supplemental Figure 2 online). The *35S:TM6* construct was expressed at similarly high levels in both the second and third whorls, as was the *35S:TAP3* construct.

We also examined the phenotypes produced by either *35S:TAP3* or *35S:TM6* in a wild-type background. In both cases, transgenic flowers displayed a wild-type phenotype.

TM6 and TAP3 Form Qualitatively Distinct Protein Complexes

In *Arabidopsis*, AP3 and PI are thought to trigger stamen development by forming a quaternary complex with the AGAMOUS (AG) and SEPALLATA3 (SEP3) MADS box proteins (Honma and Goto, 2001). AP3 and PI interact with AG indirectly through the SEP3 protein, which acts to bridge the components of the complex and also appears to provide transcriptional activation functions. The overlap of expression of AP3, PI, AG, and SEP3 in the stamens can uniquely specify stamen identity. The tomato *SEP* ortholog *TM5* is expressed in the second, third, and fourth whorls and is required for the proper differentiation of petals, stamens, and carpels (Pnueli et al., 1994). *TAG1*, the tomato *AG* ortholog, is expressed in the third and fourth whorls and specifies stamen and carpel identity (Pnueli et al., 1994).

To investigate whether *TM6* and *TAP3* have evolved divergent functions by forming different protein complexes, we performed yeast two-, three-, and four-hybrid assays to test TM6 and TAP3 protein interactions with TPI, TM5, and TAG1 (Table 3). Both TM6 and TAP3 strongly interact with TPI, suggesting that the PI protein interaction domain has been conserved between these AP3 lineage genes. We also observed that these dimers can bind to TM5. However, unlike TM6, TAP3 can bind to TM5 in the absence of TPI. The binding of the *Arabidopsis* AP3 protein to AG depends on the presence of both PI and SEP3 proteins (Honma and Goto, 2001); similarly, the tomato TAP3 protein, when expressed in conjunction with TPI and TM5, can form a quaternary complex with TAG1 (Table 3). The fact that TAG1AD-TM5+TM6BD-TPI or TAG1AD-TM5+TPIBD-TM6 does not show a positive interaction in yeast suggests that TM6 cannot replace TAP3 in the quaternary complex (Table 3). Furthermore, the positive interactions of TAG1-TM5AD+TM6BD-TPI and TAG1-TM5AD+TPIBD-TM6 can be explained by the interaction of TM5 with TM6 and TPI (Table 3). These results suggest that TM6 and TAP3 have diverged in some of their protein interaction capabilities. Furthermore, our results show that the tomato *TM5* gene, unlike the *Arabidopsis SEP3* gene (Honma and Goto, 2001), does not appear to have an intrinsic transcriptional activation domain in yeast, although we cannot exclude the possibility that TM5 does possess such activity in planta.

DISCUSSION

TAP3 and *TM6* Have Divergent and Partially Redundant Functions

To define the relative contributions of *AP3* lineage members to petal and stamen identity specification in tomato, we investigated the roles of the *TM6* and *TAP3* genes. Through the identification of a complete loss-of-function insertional mutation, we have shown that *TAP3* is required to specify petal and stamen identities. In the *tap3* loss-of-function mutant, we observed a dramatic conversion of petals to sepal-like structures as well as a homeotic conversion of stamens to carpel-like organs. The *tap3* mutation we have identified differs in some respects from *stamenless* (*sl*), a mutation that has been postulated to be an allele of *TAP3* (Gomez et al., 1999). *sl* is a semidominant and temperature-sensitive mutant; homozygous *sl* mutants grown at the restrictive temperature display a phenotype similar to the one we have described for *tap3*. One possibility is that *sl* represents a neomorphic mutation in the *TAP3* locus.

In contrast with the *tap3* loss-of-function mutant, the RNAi-induced loss of *TM6* function results in defects predominantly in stamen development. The TM6i lines show a homeotic conversion of stamens to carpel-like organs, with concomitant formation of ectopic ovules (Figures 3W to 3Z). The TM6i lines do not display any homeotic defects in petal development; the only phenotypic effect we could observe for the downregulation of *TM6* activity in petals was a reduction in overall petal size, likely caused by a reduction in cell proliferation (Table 2). Similarly, *PTD*, the *Populus trichocarpa TM6* ortholog, has been postulated to play a role in regulating cell proliferation (Sheppard et al., 2000). Although the levels of endogenous *TM6* are strongly

Table 3. In Vitro Protein Interaction Assays Reveal That TAP3 Forms Qualitatively Distinct Protein Complexes Compared with TM6

	TM6BD	TAP3BD	TPIBD	TAG1BD	TM5BD	TM6BD-TPI	TPIBD-TM6	TAP3BD-TPI	BD
TM6AD	−	−	++	−	−	n	n	−	−
TAP3AD	−	−	++	−	−	−	−	n	−
TPIAD	++	++	−	−	−	n	n	n	−
TAG1AD	−	−	−	−	−	−	−	+	−
TM5AD	−	++	−	−	−	++	++	++	−
TAG1AD-TM5	−	−	−	n	n	−	−	+	−
TM5AD-TAG1	−	+	−	n	n	++	+	+	−
AD	−	−	−	−	−	−	−	−	−

AD, Gal4 activation domain; BD, Gal4 binding domain; +, moderate interaction; ++, strong interaction; −, no interaction; n, not tested.

downregulated in the TM6i lines (Figure 2), we cannot exclude the possibility that the lack of a homeotic phenotype in petals is the result of low-level residual expression in these lines. Because *TAP3* and *TM6* do not appear to regulate each other's expression at the transcriptional level (Figure 2E), these observations suggest that *TAP3* and *TM6* have acquired developmentally distinct roles in reproductive development.

It is also clear, however, that there are some similarities in the functions of the *TAP3* and *TM6* gene products. Our experiments (Figure 5) demonstrate that when these genes are expressed in an equivalent manner, they confer a similar, but not identical, degree of rescue to the *tap3* mutant, indicating that *TM6* can substitute for some aspects of *TAP3* function.

Differing Expression Patterns of *TAP3* and *TM6* Can Partially Explain Their Divergent Functions

The tomato *AP3* paralogs show quite divergent expression patterns. *TAP3* is expressed strongly in the incipient and developing petal and stamen primordia until late stages, when its expression becomes restricted to various floral tissues (Figure 4). At early stages of flower development, *TM6* is expressed weakly but fairly ubiquitously in petal, stamen, and carpel primordia. This expression pattern shifts such that by stage 9, strong *TM6* expression is observed in developing ovules and in the transmitting tract.

The *Petunia TM6* and *DEF* genes have also been shown to be regulated differently in that Ph *TM6* is negatively regulated by the *Petunia* A-function *BLIND* gene but *BLIND* does not regulate the expression of Ph *DEF* (Tsuchimoto et al., 1993; Vandenbussche et al., 2004). An A-function gene has been identified in tomato, *MADS-MC* (Vrebalov et al., 2002); it is possible that this gene also differentially regulates the expression of the *AP3* paralogs in tomato.

Over the course of angiosperm evolution, the expression patterns of the *AP3* lineage members display some variability, indicating divergence in gene regulation (Kramer and Irish, 1999; Irish, 2003; Zahn et al., 2005). Even within the Solanaceae, there are detectable differences in orthologous gene expression patterns. For instance, the *Nicotiana benthamiana euAP3* gene, *DEF*, is expressed at high levels in the second and third whorls, but expression is detectable in all four whorls (Liu et al., 2004). This broader pattern of expression is also seen for the *Nicotiana tabacum euAP3* ortholog, *DEF* (Davies et al., 1996a). By contrast, expression of the tomato *TAP3* (Figures 2E and 4) and *Petunia DEF* genes is only detectable in the second and third whorls (Angenent et al., 1995). Also, the pattern of *TM6* expression that we describe is quite similar to that of *Petunia* Ph *TM6*, which is initially expressed in petal, stamen, and carpel primordia, becomes predominant in stamens, and at later stages is expressed strongly in the developing placenta and ovules (Vandenbussche et al., 2004).

Furthermore, our observations suggest that *TAP3*, *TM6*, and *TPI* do not regulate each other's expression to a significant degree (Figure 2E). This is quite distinct from what has been observed for *Arabidopsis* and *Antirrhinum*, in which the *PI* and *euAP3* genes cross-regulate each other's transcription to maintain continued expression (Jack et al., 1992; Trobner et al., 1992; Goto and Meyerowitz, 1994). In *Petunia*, the complete loss of *PI* lineage gene function in the *phglo1 phglo2* double mutant results in the downregulation of *DEF* but not of *TM6* (Vandenbussche et al., 2004), indicating differential regulation of the *Petunia AP3* lineage genes. Together, these observations imply that the regulation of *AP3* family members has diverged extensively. Furthermore, *euAP3* lineage genes appear to be cross-regulated differently in tomato compared with *Petunia*. It is possible that, during the evolution of the Solanaceae, this mode of cross-regulation was lost from the lineage leading to modern-day tomato.

By ectopically overexpressing *TAP3* and *TM6*, we showed that these genes could provide similar degrees of rescue to the *tap3* mutant (Figure 5). These observations suggest that the differences in the patterns of expression of these paralogous genes are responsible for much of their difference in function. Although *TM6* and *TAP3* are both expressed in petals and stamens, they appear to be expressed at different levels and in different subpopulations of cells (Figure 4), which could explain their differences in function. We did observe some subtle differences in the degree to which rescue was affected, indicating that changes in protein-coding capabilities also are likely to play a role in specifying functional differences. Together, these observations suggest that regulatory changes play a prominent role in the diversification of *TAP3* and *TM6* function.

Differences in Protein–Protein Interactions: Neofunctionalization of *euAP3*?

In *Arabidopsis*, the specific amino acid residues responsible for interactions between AP3 and PI have been mapped to the K regions of these proteins; particularly important are Glu-97 and Asp-98 in PI and Asp-98 and Arg-102 in AP3 (Yang et al., 2003). These residues are conserved in the tomato TAP3 and TM6 proteins, suggesting that their interaction with TPI may be mediated by the same protein domains. However, our data show that, at least in yeast, TM6 and TAP3 have unique as well as shared protein interaction properties that likely contribute to their distinct developmental roles. These observations support the idea that the very different C-terminal domains possessed by these proteins may be important in the formation of different protein complexes, and in turn in their different biological activities. Differences in heterodimerization capabilities have also been reported for the petunia DEF and TM6 proteins; DEF interacts with both GLO1 (FBP1) and GLO2 (pMADS2), whereas TM6 interacts strongly only with GLO2 (Vandenbussche et al., 2004). In tomato, we have isolated one *PI* ortholog gene, *TPI*, whose coding sequence is more similar to that of GLO2 than GLO1. We cannot exclude the possibility that a second PI otholog, similar to GLO1, is present in tomato and may preferentially interact with TAP3.

Analyses of synonymous versus nonsynonymous substitution rates (Goldman and Yang, 1994) of *euAP3* and *TM6* lineage coding sequences also support the idea that these paralogous lineages have evolved different roles (G. de Martino and V. F. Irish, unpublished data). Pair-wise comparisons of the full-length coding sequences of five *euAP3* genes indicate that, in all cases, the ratio of nonsynonymous to synonymous substitutions (K_a:K_s) are much less than 1. Similarly, K_a:K_s ratios for five *TM6* lineage

members are also all much less than 1. These observations indicate that each of these gene lineages is experiencing strong purifying selection, suggesting that characteristic lineage-specific residues contribute to differences in function.

TAP3 may have evolved new functions by interacting with different cofactors. For instance, the fact that TAP3 can complex with TAG1 could potentially be responsible for at least some of the differences seen between TAP3 and TM6 functions in the third whorl.

It is likely that TAP3 and TM6 also have differential interactions with tomato A-function gene products; however, the only tomato A-function gene characterized to date, *MADS-MC*, is not expressed in petal primordia (Vrebalov et al., 2002) and so likely does not participate in biologically relevant interactions with either of the tomato *AP3* paralogs. However, another tomato MADS box gene that is closely related to *MADS-MC* has been identified (Litt and Irish, 2003) and may play such a regulatory role.

We have also shown that overexpression of *TM6* can trigger petal development in the *tap3* mutant, indicating that TM6 can replace TAP3 in petal-specific protein complexes. Similarly, the maize (*Zea mays*) *paleoAP3* homolog, *SILKY1*, is able to rescue both petals and stamens in the *Arabidopsis ap3* mutant when highly overexpressed (Whipple et al., 2004). By contrast, a chimeric *Arabidopsis AP3* gene containing a *paleoAP3* C-terminal motif has been shown to rescue only the *ap3* third whorl phenotype (Lamb and Irish, 2003). These discrepancies may result from differing levels of transgene expression. Together, these observations suggest that, when highly overexpressed, AP3 lineage proteins that contain the paleoAP3 motif can replace euAP3 functions. In turn, these observations imply that the differences between paleoAP3 and euAP3 motif functions are likely to be attributable to differences in affinity for similar partner proteins.

Were the *euAP3* Lineage Genes Recruited for the de Novo Evolution of Petals in the Core Eudicots?

Morphological and paleontological data support the idea that core eudicot petals arose as an evolutionary innovation and are nonhomologous with petals from other angiosperm lineages (Takhtajan, 1991; Drinnan et al., 1994; Ronse de Craene, 2004). We have previously suggested that the advent of the divergent *euAP3* lineage genes may be correlated with this de novo evolution of petals in the core eudicots (Kramer and Irish, 1999, 2000; Irish, 2003; Lamb and Irish, 2003). The divergence in tomato *TAP3* and *TM6* gene functions can be attributed to changes in both the *cis*-regulatory and coding sequences. Together, the functional analyses of the *euAP3* and *TM6* lineage members in *Petunia* (Rijpkema et al., 2006) and tomato (this work) support the correlation of *euAP3* function with the de novo derivation of petals in the core eudicot species, in that the *euAP3* lineage gene in both cases plays a homeotic role in specifying petals. The role of the *TM6* lineage genes appears to be more variable, though, and may reflect the gradual dispensability of this gene lineage in the core eudicots. In fact, *Arabidopsis* lacks a *TM6* representative (Lamb and Irish, 2003), illustrating that, at least in this species, *TM6* function is not necessary.

The situation in noncore eudicot species may reflect a different mechanism whereby *AP3* lineage genes have acquired new roles. For instance, in monocots such as rice (*Oryza sativa*) and maize, the *paleoAP3* representatives are involved in specifying both lodicule and stamen identity (Kang et al., 1998; Moon et al., 1999; Ambrose et al., 2000). This would suggest that, within the grass lineages, *paleoAP3* genes have been recruited for the development of the grass-specific organ, the lodicule. The observation of *paleoAP3* function in grasses, combined with the analyses of *euAP3* and *TM6* gene function in core eudicots, supports a model in which, in different angiosperm clades, different mechanisms have been used to expand the roles of these genes. In core eudicots, the duplication resulting in the *euAP3* genes allowed for the recruitment of these genes to a role in petal specification; in the grasses, changes in the domain of expression of the *paleoAP3* genes appear to be responsible for their new roles in lodicule specification.

Plasticity in Evolution

Through the analyses presented here and by Rijpkema et al. (2006), we have demonstrated the functional roles of *euAP3* and *TM6* lineage genes in different members of the Solanaceae. Two paralogous *AG*-related gene lineages have also been identified in the core eudicots, resulting in the *AG* and *PLE* gene lineages (Davies et al., 1999; Nitasaka, 2003; Kramer et al., 2004; Irish and Litt, 2005). Comparisons of the functions of the *AG* and *PLE* genes in *Antirrhinum* and *Arabidopsis* suggest that these gene lineages have swapped roles (Liljegren et al., 2000; Pinyopich et al., 2003; Causier et al., 2005). However, because only two species have been functionally analyzed for *AG*/*PLE* roles, it remains unclear when the paralogous gene lineages took on complementary roles. One extreme possibility is that the duplication event resulting in the *AG* and *PLE* lineages also essentially immediately resulted in the complementary and stable subfunctionalization of these genes. By contrast, our analyses of *AP3* lineage genes demonstrate that parsing of biological function can be quite plastic. It is clear that the duplication event resulting in the *euAP3* and *TM6* lineages occurred well before the diversification of the Solanaceae. Genome-level comparisons among solanaceaeous species, including tomato and *Petunia*, have shown a high level of conservation among these genomes (Rensink et al., 2005), reflecting the relatively recent divergence of these taxa ~40 million years ago (Clegg et al., 1997). Nonetheless, the *euAP3* and *TM6* gene functions have been parsed quite differently in tomato and *Petunia*, illustrating that subfunctionalization is a dynamic and fluid process.

METHODS

Phylogenetic Analyses

Sequences of *AP3* lineage genes from selected basal and core eudicots were obtained from the National Center for Biotechnology Information GenBank. The MIK domains were aligned using MacVector (Accelrys) and adjusted manually (see Supplemental Figure 1 online). The neighbor-joining analysis was performed and bootstrapped 2000 times using PAUP*b10 (Swofford, 2000).

In Situ Hybridizations

In situ hybridizations were performed according to published protocols (Jackson, 1991) with minor modifications. Tomato (*Solanum lycopersicum* cv Micro-Tom) wild-type floral buds were fixed in 4% paraformaldehyde in PBS and embedded in Paraplast Plus tissue-embedding medium (Tyco Healthcare). For the *TAP3* antisense probe, a 563-bp probe was made using the TAP3F primer (5′-TTGTTCGATCTGTACCAGAAG-3′) and the TAP3RT7 primer containing the T7 promoter (5′-CATAATACGACTCACTATAGGGTTCTTGTGAACAAACATTGC-3′). For the *TM6* antisense probe, a 909-bp probe was made using the TM6F primer (5′-AAGAAGATTGAAAACTTGAC-3′) and the TM6RT7 primer containing the T7 promoter (5′-CATAATACGACTCACTATAGGGTAAGTCGAAAAGGAAAATTG-3′). For the *TPI* antisense probe, a 400-bp probe was made using the TPIF primer (5′-CAATCAACTTACCCATAAAGAGC-3′) and the TPIRT7 primer containing the T7 promoter (5′-CATAATACGACTCACTATAGGGCCAACATGAAACAGAGTCTTAGC-3′). Hybridizations were performed at 48°C, and subsequent washes were done at 52°C.

Identification of *TPI* and *TAP3* Sequences

Poly(A) mRNA was extracted from total RNA using Magnetight oligo(dT) beads (Novagen). Single-stranded cDNA was synthesized by priming with oligo(dT)$_{25}$ from 500 ng of poly(A$^+$) RNA. Two degenerate primers complementary to the K domain and the PI motif of *PI*-like genes were used to amplify the tomato PI ortholog, *TPI*, cDNA (TPIF, 5′-GGATGC(T/A)AA(G/A)CATGA(G/A)(A/C)AI(T/C)GA(A/G)ATA-3′; TPIR, 5′-TGIA(A/G)(A/G)TTIGGITGIA(A/T)(T/G)GGITG-3′).

PCR was performed using the following regime: 10 cycles of 20 s of denaturing at 94°C, 30 s of annealing at 38°C, and a 1-min extension at 72°C. The program was completed by 30 cycles of 20 s of denaturing at 94°C, 30 s of annealing at 42°C, and an extension time of 1 min at 72°C. The *TPI* cDNA full-length sequence was obtained by RACE reactions according to the manufacturer's protocol (Gibco BRL). A partial sequence of the *TAP3* gene has already been isolated (accession number AF052868). To obtain the 5′ terminus of the *TAP3* cDNA, we performed 5′ RACE reactions (primer sequences for RACE are available upon request).

Isolation of the *tap3* Loss-of-Function Mutation

Inverse PCR was performed with *Ds*-specific primers (Ds5216, 5′-TTGTATATCCCGTTTCCGTTCCGTT-3′; Ds7665, 5′-TTTCGTTTCCGTCCCGCAAGTTAAATA-3′) using genomic DNA from line EE1153, leading to the identification of an insertion in the tomato *TAP3* gene. PCR was performed using the Expand Long Template PCR system (Boehringer) with the following program: 10 cycles of 10 s of denaturing at 94°C, 30 s of annealing at 60°C, and 5 min at 68°C; 20 cycles of 10 s at 94°C, 30 s at 60°C, and 5 s + 20 s at 68°C; and a final step of 7 min at 68°C. Further screening of the individual plants by PCR using *Ds*- and *TAP3*-specific primers showed that these plants were heterozygous for the insertion (primer sequences are available upon request). Cosegregation of the Ds element and the mutant phenotype was confirmed by both DNA gel blot analyses and PCR.

Transformation Constructs and Plant Transformation

Plant transformations were all performed using cv Micro-Tom. We generated a *TM6* RNAi construct to target part of the C terminus and the 3′ untranslated region of the endogenous *TM6* transcript. A 220-bp fragment was amplified by PCR with *TM6*-specific primers (TM6-617F, 5′-CATTGCACCCCAATCTTCAAAACG-3′; TM6-837R, 5′-CAAGATCTGCTTAACACAGAACCAAATCCAGACTCG-3′). The second intron of *Arabidopsis thaliana AP3* was used for the hairpin of the double-stranded RNA. The TM6+/AP3int/TM6− construct was inserted into the binary vector pTCSH1 (Hardtke et al., 2000) in the *Xho*I/*Xba*I sites. For the *TM6* and *TAP3* overexpression constructs, the complete open reading frame of *TM6* or *TAP3* was amplified by PCR and inserted in *Xho*I/*Xba*I sites of the pTCSH1 binary vector. pTCSH1 binary vectors containing the sequence of interest were electroporated into the *Agrobacterium tumefaciens* LBA 4404 strain and used in independent tomato transformations.

Micro-Tom was transformed using a protocol derived from a previously published method (Fillatti et al., 1987) with some modifications. Seeds were germinated on Murashige and Skoog medium at 25°C under constant light. Explants of 7-d-old cotyledons were incubated for 40 min with the *Agrobacterium* LBA 4404 strain containing the construct of interest (grown to log phase). After incubation, the explants were quickly dried on sterile paper and transferred to a cocultivation medium containing 2% glucose and 100 μM acetosyringone. After 2 d of cocultivation in the dark, the explants were transferred to D1 medium containing 1 mg/L zeatin, 200 mg/L timentin, 0.05 mg/L indole-3-acetic acid, and 25 mg/L glufosinate ammonium (Sigma-Aldrich) under constant light. After 2 to 3 weeks, the regenerated calli were transferred to the same medium except that zeatin was reduced to 0.1 mg/L for shoot formation. Shoots of 1- to 1.5-cm plantlets were cut from the calli, dipped into a rooting powder solution, and transferred into soil. The T1 transgenic plants were checked for the presence of the transgene by PCR amplification of the BAR gene (BAR-F, 5′-AGACAAGCACGGTCAACTTCCGTA-3′; BAR-R, 5′-CGATGACAGCGACCACGCTCTT-3′). The T2 generation lines were selected by screening the seed progeny on Murashige and Skoog medium containing 25 mg/L glufosinate ammonium and 0.5% sucrose.

For the *tap3* rescue experiments, cotyledons from progeny of *TAP3*/*tap3* heterozygous plants were used in the transformation; homozygous mutant *tap3* transgenic plants were identified by PCR.

Scanning Electron Microscopy

Plant samples were fixed overnight in a 3:1 ethanol:glacial acetic acid solution, gradually dehydrated to 100% ethanol, and dried in a critical point drier. Samples were dissected with a stereomicroscope by removing some parts to reveal the organs to be examined. The resulting samples were analyzed using previously published protocols (Irish and Sussex, 1990).

RT-PCR

Total RNA was isolated using Trizol reagent (Life Technologies) according to the manufacturer's protocol. Five micrograms of total RNA was used as a template for first-strand cDNA synthesis in a volume of 20 μL with 1 μL of Superscript II RT (Gibco BRL). The RT reaction was diluted 1:5, and 2 μL was used for PCR. The primers used were as follows: TM61F (5′-ATGGGACGGGGAAAAATTGAGATCAAGAAGATT-3′) and TM6-570R (5′-GCAAATGCCACAGCAGAGAGTGG-3′) for *TM6*; TAP3-1F (5′-AATGGGCTATTCAAGAAGGCTAATG-3′) and TAP3-580R (5′-CACCTCCACTGTGAAGATGATTATG-3′) for *TAP3*; TPI-1F (5′-CATCATGGGGAGAGGTAAAATAG-3′) and TPI-760R (5′-GGTAATAATTCCAACATGAAACAG-3′) for *TPI*; and LEACTF (5′-CAGGATTTGCTGGTGATGCTCCTC-3′) and LEACTR (5′-GAGGTACGACCGCTAGCATACAG-3′) for *ACTIN* (accession number AB199316). The PCR regime was 25 s of denaturing at 94°C, 25 s of annealing at 56°C, and an extension time of 1 min at 72°C, with 32 cycles for the *TM6* gene and 28 cycles for the *ACTIN*, *TPI*, and *TAP3* genes.

Yeast Two-, Three-, and Four-Hybrid Analysis

TM6, TAP3, TPI, TM5, and TAG1 IKC domains were used to test protein interactions in yeast assays. For the two-hybrid analysis, single proteins were fused with the GAL4 DNA binding domain in the pGBT9 vector

(Clontech) and with the GAL4 activation domain in the pGAD424 vector (Clontech). For the three- and four-hybrid analyses, two genes on the same vector were expressed under the control of two independent ADH1 promoters. Protein interactions were confirmed by testing different vector combinations: (X − AD; Y) + (W − BD; Z), (W; Z − AD) + (X; Y − BD), etc. Two independent transformations for each vector combination were performed, and five colonies per transformation were used for the assay. The β-galactosidase liquid assay was performed using a protocol available at http://www.fhcrc.org/science/labs/gottschling/yeast/Bgal.html.

Accession Numbers

Sequences of *AP3* lineage genes from selected basal and core eudicots were obtained from GenBank: *AP3* (AF115814), *RAD1* (X89113), *RAD2* (X89108), *SLM3* (X80490), *GDEF1* (AJ009724), *GDEF2* (AJ009725), *HPDEF1* (AF180364), *HPDEF2* (AF180365), Ph *DEF* (X69946), Ph *TM6* (AF230704), Nt *DEF* (X96428), Nt *TM6* (AY577817), Le *TM6* (X60759), Le *AP3* (AF052868 and this study), *DEF* (X52023), Hm *AP3* (AF230702), Hm *TM6* (AF230703), *MASAKO B3* (AB055966), Md *TM6* (AB081093), Md *MADS13* (Aj251116), *PTD* (AF057708), Jr *AP3* (AJ313089), *NMH7* (L41727), Ri.sa. *AP3-1* (AY337758), Ri.sa. *AP3-2* (AY337759), Gu.ti. *AP3-4* (AY337756), Gu.ti. *AP3-5* (AY337757), Pn *AP3-1* (AF052873), Pn *AP3-2* (AF052874), De *AP3* (AF052875), Rb *AP3-1* (AF052876), Rb *AP3-2* (AF130869), Pc *AP3* (AF052872), Pt *AP3-1* (AF052870), Pt *AP3-2* (AF052871), *STDEF* (X67511). Sequence data from this article can be found in the GenBank data library under the following accession numbers: *TPI* (DQ674531) and *TAP3* (DQ674532).

Supplemental Data

The following materials are available in the online version of this article.

Supplemental Figure 1. Alignment Used for Phylogenetic Analyses.

Supplemental Figure 2. RT-PCR Analyses of *TAP3* and *TM6* Expression Levels.

ACKNOWLEDGMENTS

We thank Queenie Tan for her help in generating the RNAi constructs. We appreciate the kindness of Christian Hardtke and Tamara Western for providing laboratory facilities for part of this work. We thank members of the Irish laboratory and David Weiss for constructive comments on the manuscript and Tom Gerats and Michiel Vandenbussche for communicating results before publication. This work was supported by Grant 0110731 from the National Science Foundation to V.F.I.

Received April 2, 2006; revised May 12, 2006; accepted June 6, 2006; published July 14, 2006.

REFERENCES

Ambrose, B.A., Lerner, D.R., Ciceri, P., Padilla, C.M., Yanofsky, M.F., and Schmidt, R.J. (2000). Molecular and genetic analyses of the Silky1 gene reveal conservation in floral organ specification between eudicots and monocots. Mol. Cell **5,** 569–579.

Angenent, G.C., Busscher, M., Franken, J., Dons, H.J., and van Tunen, A.J. (1995). Functional interaction between the homeotic genes fbp1 and pMADS1 during petunia floral organogenesis. Plant Cell **7,** 507–516.

Benfey, P.N., and Chua, N.-H. (1990). The cauliflower mosaic virus 35S promoter: Combinatorial regulation of transcription in plants. Science **250,** 959–966.

Bowman, J.L., Smyth, D.R., and Meyerowitz, E.M. (1989). Genes directing flower development in *Arabidopsis.* Plant Cell **1,** 37–52.

Brukhin, V., Hernould, M., Gonzalez, N., Chevalier, C., and Mouras, A. (2003). Flower development schedule in tomato *Lycopersicon esculentum* cv. Sweet Cherry. Sex. Plant Reprod. **15,** 311–320.

Busi, M.V., Bustamante, C., D'Angelo, C., Hidalgo-Cuevas, M., Boggio, S.B., Valle, E.M., and Zabaleta, E. (2003). MADS-box genes expressed during tomato seed and fruit development. Plant Mol. Biol. **52,** 801–815.

Carpenter, R., and Coen, E.S. (1990). Floral homeotic mutations produced by transposon-mutagenesis in *Antirrhinum majus.* Genes Dev. **4,** 1483–1493.

Causier, B., Castillo, R., Zhou, J., Ingram, R., Xue, Y., Schwarz-Sommer, Z., and Davies, B. (2005). Evolution in action: Following function in duplicated floral homeotic genes. Curr. Biol. **15,** 1508–1512.

Clegg, M.T., Cummings, M.P., and Durbin, M.L. (1997). The evolution of plant nuclear genes. Proc. Natl. Acad. Sci. USA **94,** 7791–7798.

Davies, B., Di Rosa, A., Eneva, T., Saedler, H., and Sommer, H. (1996a). Alteration of tobacco floral organ identity by expression of combinations of Antirrhinum MADS-box genes. Plant J. **10,** 663–677.

Davies, B., Egea-Cortines, M., de Andrade Silva, E., Saedler, H., and Sommer, H. (1996b). Multiple interactions among floral homeotic MADS box proteins. EMBO J. **16,** 4330–4343.

Davies, B., Motte, P., Keck, E., Saedler, H., Sommer, H., and Schwarz-Sommer, Z. (1999). PLENA and FARINELLI: Redundancy and regulatory interactions between two Antirrhinum MADS-box factors controlling flower development. EMBO J. **18,** 4023–4034.

Drinnan, A.N., Crane, P.R., and Hoot, S.B. (1994). Patterns of floral evolution in the early diversification of non-magnoliid dicotyledons (eudicots). In Early Evolution of Flowers, P.K. Endress and E.M. Friis, eds (New York: Springer-Verlag), pp. 93–122.

Fillatti, J., Kiser, J., Rose, B., and Comai, L. (1987). Efficient transformation of tomato and the introduction and expression of a gene for herbicide tolerance. In Tomato Biotechnology, D. Nevins and R. Jones, eds (New York: Alan R. Liss), pp. 199–210.

Force, A., Lynch, M., Pickett, F.B., Amores, A., Yan, Y.L., and Postlethwait, J. (1999). Preservation of duplicate genes by complementary, degenerative mutations. Genetics **151,** 1531–1545.

Goldman, N., and Yang, Z. (1994). A codon-based model of nucleotide substitution for protein-coding DNA sequences. Mol. Biol. Evol. **11,** 725–736.

Gomez, P., Jamilena, M., Capel, J., Zurita, S., Angosto, T., and Lozano, R. (1999). Stamenless, a tomato mutant with homeotic conversions in petals and stamens. Planta **209,** 172–179.

Goto, K., and Meyerowitz, E.M. (1994). Function and regulation of the Arabidopsis floral homeotic gene PISTILLATA. Genes Dev. **8,** 1548–1560.

Halfter, U., Ali, N., Stockhaus, J., Ren, L., and Chua, N.-H. (1994). Ectopic expression of a single homeotic gene, the Petunia gene green petal, is sufficient to convert sepals to petaloid organs. EMBO J. **13,** 1443–1449.

Hardtke, C.S., Gohda, K., Osterlund, M.T., Oyama, T., Okada, K., and Deng, X.W. (2000). HY5 stability and activity in Arabidopsis is regulated by phosphorylation in its COP1 binding domain. EMBO J. **19,** 4997–5006.

Honma, T., and Goto, K. (2000). The Arabidopsis floral homeotic gene PISTILLATA is regulated by discrete cis-elements responsive to induction and maintenance signals. Development **127,** 2021–2030.

Honma, T., and Goto, K. (2001). Complexes of MADS-box proteins are sufficient to convert leaves into floral organs. Nature **409,** 469–471.

Irish, V.F. (2003). The evolution of floral homeotic gene function. Bioessays **25,** 637–646.

Irish, V.F., and Kramer, E.M. (1998). Genetic and molecular analysis of angiosperm flower development. Adv. Bot. Res. **28,** 197–230.

Irish, V.F., and Litt, A. (2005). Flower development and evolution: Gene duplication, diversification and redeployment. Curr. Opin. Genet. Dev. **15,** 454–460.

Irish, V.F., and Sussex, I.M. (1990). Function of the apetala-1 gene during Arabidopsis floral development. Plant Cell **2,** 741–753.

Jack, T., Brockman, L.L., and Meyerowitz, E.M. (1992). The homeotic gene APETALA3 of *Arabidopsis thaliana* encodes a MADS box and is expressed in petals and stamens. Cell **68,** 683–697.

Jack, T., Fox, G.L., and Meyerowitz, E.M. (1994). Arabidopsis homeotic gene APETALA3 ectopic expression: Transcriptional and posttranscriptional regulation determine floral organ identity. Cell **76,** 703–716.

Jackson, D. (1991). In situ hybridisation in plants. In Molecular Plant Pathology: A Practical Approach, D.J. Bowles, S.J. Gurr, and P. McPherson, eds (Oxford, UK: Oxford University Press), pp. 163–174.

Kang, H.-G., Jeon, J.-S., Lee, S., and An, G. (1998). Identification of class B and class C floral organ identity genes from rice plants. Plant Mol. Biol. **38,** 1021–1029.

Kim, S., Yoo, M., Albert, V.A., Farris, J.S., Soltis, P.S., and Soltis, D.E. (2004). Phylogeny and diversification of B-function genes in angiosperms: Evolutionary and functional implications of a 260-million year old duplication. Am. J. Bot. **91,** 2102–2118.

Kramer, E.M., Dorit, R.L., and Irish, V.F. (1998). Molecular evolution of petal and stamen development: Gene duplication and divergence within the APETALA3 and PISTILLATA MADS-box gene lineages. Genetics **149,** 765–783.

Kramer, E.M., and Irish, V.F. (1999). Evolution of genetic mechanisms controlling petal development. Nature **399,** 144–148.

Kramer, E.M., and Irish, V.F. (2000). Evolution of petal and stamen developmental programs: Evidence from comparative studies of the lower eudicots and basal angiosperms. Int. J. Plant Sci. **161** (suppl.), S29–S40.

Kramer, E.M., Jaramillo, M.A., and Di Stilio, V.S. (2004). Patterns of gene duplication and functional evolution during the diversification of the AGAMOUS subfamily of MADS box genes in angiosperms. Genetics **166,** 1011–1023.

Kramer, E.M., Su, H.J., Wu, C.C., and Hu, J.M. (2006). A simplified explanation for the frameshift mutation that created a novel C-terminal motif in the APETALA3 gene lineage. BMC Evol. Biol. **6,** 30.

Lamb, R.S., and Irish, V.F. (2003). Functional divergence within the APETALA3/PISTILLATA floral homeotic gene lineages. Proc. Natl. Acad. Sci. USA **100,** 6558–6563.

Liljegren, S.J., Ditta, G.S., Eshed, Y., Savidge, B., Bowman, J.L., and Yanofsky, M.F. (2000). SHATTERPROOF MADS-box genes control seed dispersal in Arabidopsis. Nature **404,** 766–770.

Litt, A., and Irish, V.F. (2003). Duplication and diversification in the APETALA1/FRUITFULL floral homeotic gene lineage: Implications for the evolution of floral development. Genetics **165,** 821–833.

Liu, Y., Nakayama, N., Schiff, M., Litt, A., Irish, V.F., and Dinesh-Kumar, S.P. (2004). Virus induced gene silencing of a DEFICIENS ortholog in *Nicotiana benthamiana.* Plant Mol. Biol. **54,** 701–711.

Lozano, R., Angosto, T., Gomez, P., Payan, C., Capel, J., Huijser, P., Salinas, J., and Martinez-Zapater, J.M. (1998). Tomato flower abnormalities induced by low temperatures are associated with changes of expression of MADS-box genes. Plant Physiol. **117,** 91–100.

Lynch, M., and Conery, J.S. (2000). The evolutionary fate and consequences of duplicate genes. Science **290,** 1151–1155.

Lynch, M., and Force, A. (2000). The probability of duplicate gene preservation by subfunctionalization. Genetics **154,** 459–473.

Magallon, S., Crane, P.R., and Herendeen, P.S. (1999). Phylogenetic pattern, diversity, and diversification of eudicots. Ann. Mo. Bot. Gard. **86,** 297–372.

McGonigle, B., Bouhidel, K., and Irish, V.F. (1996). Nuclear localization of the Arabidopsis APETALA3 and PISTILLATA homeotic gene products depends on their simultaneous expression. Genes Dev. **10,** 1812–1821.

Meissner, R., Chague, V., Zhu, Q., Emmanuel, E., Elkind, Y., and Levy, A.A. (2000). A high throughput system for transposon tagging and promoter trapping in tomato. Plant J. **22,** 265–274.

Meissner, R., Jacobson, Y., Melamed, S., Levyatuv, S., Shalev, G., Ashri, A., Elkind, Y., and Levy, A. (1997). A new model system for tomato genetics. Plant J. **12,** 1465–1472.

Moon, Y.H., Jung, J.Y., Kang, H.G., and An, G. (1999). Identification of a rice APETALA3 homologue by yeast two-hybrid screening. Plant Mol. Biol. **40,** 167–177.

Nitasaka, E. (2003). Insertion of an En/Spm-related transposable element into a floral homeotic gene DUPLICATED causes a double flower phenotype in the Japanese morning glory. Plant J. **36,** 522–531.

Ohno, S. (1970). Evolution by Gene Duplication. (New York: Springer).

Pelaz, S., Tapia-Lopez, R., Alvarez-Buylla, E.R., and Yanofsky, M.F. (2001). Conversion of leaves into petals in Arabidopsis. Curr. Biol. **11,** 182–184.

Pinyopich, A., Ditta, G.S., Savidge, B., Liljegren, S.J., Baumann, E., Wisman, E., and Yanofsky, M.F. (2003). Assessing the redundancy of MADS-box genes during carpel and ovule development. Nature **424,** 85–88.

Pnueli, L., Abu-Abeid, M., Zamir, D., Nacken, W., Schwarz-Sommer, Z., and Lifschitz, E. (1991). The MADS box gene family in tomato: Temporal expression during floral development, conserved secondary structures and homology with homeotic genes from *Antirrhinum* and *Arabidopsis.* Plant J. **1,** 255–266.

Pneuli, L., Hareven, D., Broday, L., Hurwitz, C., and Lifshitz, E. (1994). The TM5 MADS box gene mediates organ differentiation in the three inner whorls of tomato flowers. Plant Cell **6,** 175–186.

Pnueli, L., Hareven, D., Rounsley, S.D., Yanofsky, M.F., and Lifschitz, E. (1994). Isolation of the tomato AGAMOUS gene TAG1 and analysis of its homeotic role in transgenic plants. Plant Cell **6,** 163–173.

Rensink, W.A., Lee, Y., Liu, J., Iobst, S., Ouyang, S., and Buell, C.R. (2005). Comparative analyses of six solanaceous transcriptomes reveal a high degree of sequence conservation and species-specific transcripts. BMC Genomics **6,** 124.

Riechmann, J.L., Krizek, B.A., and Meyerowitz, E.M. (1996a). Dimerization specificity of Arabidopsis MADS domain homeotic proteins APETALA1, APETALA3, PISTILLATA, and AGAMOUS. Proc. Natl. Acad. Sci. USA **93,** 4793–4798.

Riechmann, J.L., Wang, M., and Meyerowitz, E.M. (1996b). DNA-binding properties of Arabidopsis MADS domain homeotic proteins APETALA1, APETALA3, PISTILLATA and AGAMOUS. Nucleic Acids Res. **24,** 3134–3141.

Rijpkema, A., Royaert, S., Zethof, J., van der Weerden, G., Gerats, T., and Vandenbussche, M. (2006). Functional divergence within the DEF/AP3 lineage: An analysis of PhTM6 in *Petunia hybrida.* Plant Cell **18,** 1819–1832.

Ronse de Craene, L.P. (2004). Floral development of *Berberidopsis corallina*: A crucial link in the evolution of flowers in the core eudicots. Ann. Bot. (Lond.) **94,** 741–751.

Schwarz-Sommer, Z., Hue, I., Huijser, P., Flor, P.J., Hansen, R., Tetens, F., Lonnig, W.-E., Saedler, H., and Sommer, H. (1992). Characterization of the *Antirrhinum* floral homeotic MADS-box gene *deficiens*: Evidence for DNA binding and autoregulation of its persistent expression throughout flower development. EMBO J. **11,** 251–263.

Sekhar, K.N.C., and Sawhney, V.K. (1984). A scanning electron microscope study of the development and surface features of floral organs of tomato (*Lycopersicon esculentum*). Can. J. Bot. **62,** 2403–2413.

Sheppard, L.A., Brunner, A.M., Krutovskii, K.V., Rottmann, W.H., Skinner, J.S., Vollmer, S.S., and Strauss, S.H. (2000). A DEFICIENS homolog from the dioecious tree black cottonwood is expressed in female and male floral meristems of the two-whorled unisexual flowers. Plant Physiol. **124,** 627–640.

Sommer, H., Beltran, J.-P., Huijser, P., Pape, H., Lonnig, W.-E., Saedler, H., and Schwarz-Sommer, Z. (1990). *Deficiens*, a homeotic gene involved in the control of flower morphogenesis in *Antirrhinum majus*: The protein shows homology to transcription factors. EMBO J. **9,** 605–613.

Stellari, G.M., Jaramillo, M.A., and Kramer, E.M. (2004). Evolution of the APETALA3 and PISTILLATA lineages of MADS-box-containing genes in the basal angiosperms. Mol. Biol. Evol. **21,** 506–519.

Swofford, D.L. (2000). PAUP*: Phylogenetic Analysis Using Parsimony (and Other Methods). (Sunderland, MA: Sinauer Associates).

Takhtajan, A. (1991). Evolutionary Trends in Flowering Plants. (New York: Columbia University Press).

Theissen, G., Becker, A., Di Rosa, A., Kanno, A., Kim, J.T., Muenster, T., Winter, K.-W., and Saedler, H. (2000). A short history of MADS-box genes in plants. Plant Mol. Biol. **42,** 115–149.

Theissen, G., and Saedler, H. (2001). Plant biology. Floral quartets. Nature **409,** 469–471.

Trobner, W., Ramirez, L., Motte, P., Hue, I., Huijser, P., Lonnig, W.E., Saedler, H., Sommer, H., and Schwarz-Sommer, Z. (1992). Globosa—A homeotic gene which interacts with Deficiens in the control of Antirrhinum floral organogenesis. EMBO J. **11,** 4693–4704.

Tsuchimoto, S., Mayama, T., van der Krol, A., and Ohtsubo, E. (2000). The whorl-specific action of a petunia class B floral homeotic gene. Genes Cells **5,** 89–99.

Tsuchimoto, S., van der Krol, A.R., and Chua, N.-H. (1993). Ectopic expression of pMADS3 in transgenic petunia phenocopies the petunia blind mutant. Plant Cell **5,** 843–853.

Vandenbussche, M., Theissen, G., Van de Peer, Y., and Gerats, T. (2003). Structural diversification and neo-functionalization during floral MADS-box gene evolution by C-terminal frameshift mutations. Nucleic Acids Res. **31,** 4401–4409.

Vandenbussche, M., Zethof, J., Royaert, S., Weterings, K., and Gerats, T. (2004). The duplicated B-class heterodimer model: Whorl-specific effects and complex genetic interactions in *Petunia hybrida* flower development. Plant Cell **16,** 741–754.

van der Krol, A.R., Brunelle, A., Tsuchimoto, S., and Chua, N.H. (1993). Functional analysis of petunia floral homeotic MADS box gene pMADS1. Genes Dev. **7,** 1214–1228.

Vrebalov, J., Ruezinsky, D., Padmanabhan, V., White, R., Medrano, D., Drake, R., Schuch, W., and Giovannoni, J. (2002). A MADS-box gene necessary for fruit ripening at the tomato ripening-inhibitor (rin) locus. Science **296,** 343–346.

Whipple, C.J., Ciceri, P., Padilla, C.M., Ambrose, B.A., Bandong, S.L., and Schmidt, R.J. (2004). Conservation of B-class floral homeotic gene function between maize and Arabidopsis. Development **131,** 6083–6091.

Yang, Y., Fanning, L., and Jack, T. (2003). The K domain mediates heterodimerization of the Arabidopsis floral organ identity proteins, APETALA3 and PISTILLATA. Plant J. **33,** 47–59.

Zahn, L.M., Leebens-Mack, J., DePamphilis, C.W., Ma, H., and Theissen, G. (2005). To B or not to B a flower: the role of DEFICIENS and GLOBOSA orthologs in the evolution of the angiosperms. J. Hered. **96,** 225–240.